

String theory in Lorentz-invariant light cone gauge - III

Igor Nikitin, Lialia Nikitina

Fraunhofer Society, IMK.VE, 53754, St.Augustin, Germany

This paper completes the work, initiated in [1, 2], further referred as Parts I and II, concerning to Dirac's quantization of Nambu-Goto theory of open string, formulated in the space-time of dimension $d = 4$. Here we perform more detailed study of Gribov's copies in the classical mechanics and determine the quantum spectrum of masses for the arbitrary spin case.

1 Gribov's copies

Gribov's copies are multiple intersections of the orbit of gauge group and the surface of gauge fixing condition. In Part II we have shown that the considered version of string theory possesses Gribov's copies, related with the singular points of a specially constructed vector field on the sphere. Therefore, the following topological invariants can be introduced for Gribov's copies.

Definition 1: let the phase space M be a smooth orientable manifold. Let the orbit of gauge group G and the surface of gauge fixing condition F be its smooth orientable submanifolds with $\dim(G) = \text{codim}(F)$. Let P be the point of their transversal intersection. This means that in point P the tangent spaces to G and F span the tangent space to M . Let $\vec{\tau}(F, P)$, $\vec{\tau}(G, P)$ and $\vec{\tau}(M, P)$ be the bases in the tangent spaces, defining the orientation of F , G and M , evaluated in point P . The *index of intersection* of F and G in point P is defined as a number ν , equal to $(+1)$ if the basis $(\vec{\tau}(F, P), \vec{\tau}(G, P))$ has the same orientation as the basis $\vec{\tau}(M, P)$, and equal to (-1) if the orientations are opposite.

Definition 2: non-degenerate singular points of 2-dimensional vector field are focus, center, node and saddle. Standard topological classification introduces the *index of singular point* ν , equal to $(+1)$ for the cases (focus, center, node) and equal to (-1) for the saddle.

Lemma 1 (*topological charges of Gribov's copies*): these two definitions coincide.

The explicit expressions for the vector fields are given by Eq.(12) in Part II. There is also an alternative definition:

$$\vec{a}_n = \frac{1}{2\sqrt{2\pi}} \oint d\vec{Q}(\sigma) \cdot \exp \left[\frac{2\pi i n}{L_t} (L(\sigma) - (\vec{Q}(\sigma) - \vec{X})\vec{e}_3) \right], \quad (1)$$

where $\vec{X} = \oint dL(\sigma)\vec{Q}(\sigma)/L_t$ defines an average position of the curve $\vec{Q}(\sigma)$ and coincides with the definition of mean coordinate in CMF given in Part I. The difference of (1) and PII-Eq.(12) consists in \vec{e}_3 -dependent phase factor $e^{in\varphi(\vec{e}_3)}$, $\varphi(\vec{e}_3) = 2\pi(\vec{X} - \vec{Q}(0))\vec{e}_3/L_t$. According to the Part II, the evolution of \vec{a}_n is the phase rotation. Thus, the phase factor actually introduces a difference of "local time" for the evolution of vector fields on the sphere.

Lemma 2 (*phase factor*): the factor $e^{in\varphi(\vec{e}_3)}$ preserves the orbits of Gribov's copies and changes their evolution parameter from lcg's PII-Eq.(13) to the natural one (length of the curve).

Further we will use the definition (1), more convenient to study the evolution of Gribov's copies.

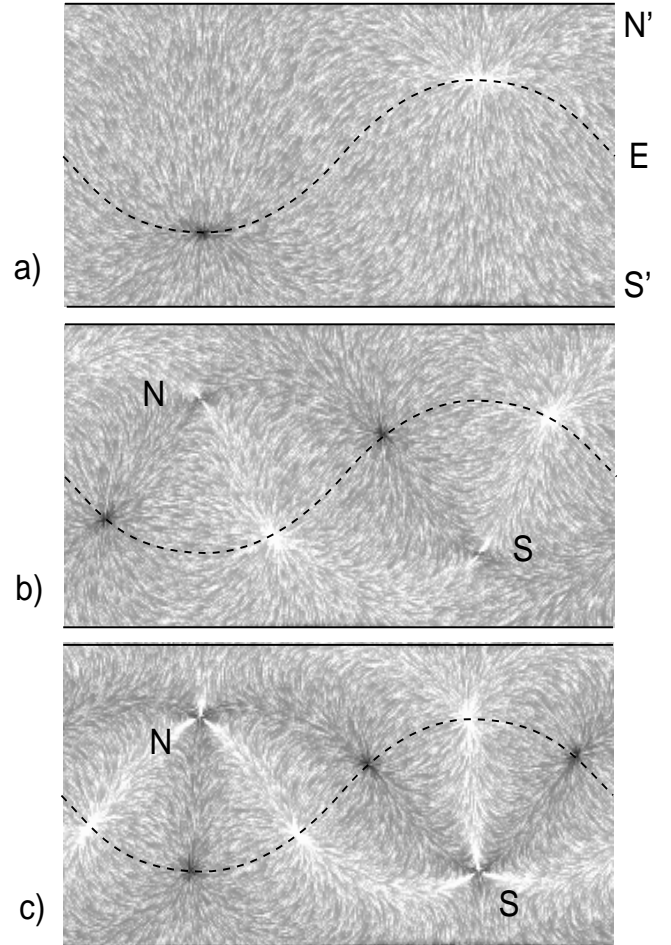


Fig.1. Gribov's copies. These images are created by a computer program for the visualization of vector fields, courtesy of Wasil Urazmetov, IHEP, Protvino, Russia. A paper on the visualization techniques used in this program will be published elsewhere.

To investigate the properties of Gribov's copies in more detail, we perform their visualization. The vector fields of fig.1 are displayed on a spherical map (longitude, latitude), where the top and bottom lines correspond to auxiliary poles N', S' . These poles are specially selected in regular

points of the vector field, to prevent the image distortion in the vicinity of the original poles N,S, where the singularities are located. The equator E for the poles N,S is shown on the images by dashed line. The following singularities of the vector field are visible in these images: nodes – as spots of black/white color, dependent on the field direction (source/sink); saddles – as cross-shaped black-white spots with a hyperbolic structure of the field in the vicinity. The visualization allows to formulate the following lemma (analytically proven in Appendix 1).

Lemma 3 (*nearly straight solution, analog of PII-L5,6*):

For the straight line string the singular points of the vector field $\vec{q}_{s\perp}(\vec{e}_3)$ are: at $s = 1$ two nodes on the equator (fig.1a), at $s = 2$ saddles on the northern and southern poles and four nodes on the equator (fig.1b), at $s > 2$ multi-saddles on the northern and southern poles and $2s$ nodes on the equator ($s = 3$, fig.1c). During the evolution the nodes move along the equator, while the singular points in the poles stay fixed and saddle patterns rotate around them. After a small deformation of the string from straight configuration the nodes move along a common trajectory in the vicinity of the equator; at $s = 2$ the saddles move in small loops near the poles; at $s > 2$ the multi-saddles are unfolded to $(s - 1)$ non-degenerate saddles moving near the poles. After the lapse of time $\Delta\tau_s = \pi/s = (\text{period of evolution})/2s$ the vector field reverses its direction and the pattern of singularities returns to the initial state. During this time the equatorial singularities move to the neighbor ones, pole singularities at $s = 2$ perform one revolution along the loops.

The discussion of the properties of Gribov's copies in quantum theory can be found in Appendix 3.

2 Arbitrary spin case

2.1 Classical mechanics

Let's define $\gamma = (L_0^{(2)})^{-1/2}$.

Lemma 4 (*structural, analog of PII-L2*): a_2 expansion in the vicinity of straight-line string has a form

$$a_2 = \sum_{n \geq 1} \frac{P_n a_1^2}{|a_1|^{4n}}, \quad (2)$$

where P_n are polynomials of $a_1, \Sigma_-, S_-, d, f, g'$, their conjugates and γ, γ^{-1} . The polynomials possess the following properties: (i) each monomial in P_n contains, counting powers, n variables from the group $(\Sigma_-, S_-, d, f, g'$ and their conjugates) and $2(n - 1)$ variables from the group (a_1, a_1^*) ; (ii) each monomial contains at least one variable from the group (Σ_{\pm}, S_{\pm}) ; (iii) variables a_1 and a_1^* enter in even powers only; (iv) each monomial, containing S_- , also contains $(a_1^*)^{2k}$ with $k \geq 1$; (v) $P_n = O(\gamma^{-[(n+1)/2]})$ at $\gamma \rightarrow 0$.

For the purposes of further consideration it is convenient to extract from a_2 a common phase multiplier $a_1^2/|a_1|^2$ and to define $a_2 = \alpha_2 \cdot a_1^2/|a_1|^2$, so that $|a_2| = |\alpha_2|$ and

$$\alpha_2 = \sum_{n \geq 1} \frac{P_n}{|a_1|^{4n-2}}, \quad \frac{P^2}{2\pi} = L_0^{(2)} + 2|\alpha_2|^2. \quad (3)$$

Explicit expressions for the first three polynomials P_n are:

$$P_1 = -\Sigma_+ + S_+/\gamma,$$

$$P_2 = a_1^{*2} f^* \Sigma_- + a_1^2 g'^* \Sigma_+ - a_1^{*2} f^* S_-/\gamma - a_1^2 g'^* S_+/\gamma,$$

$$P_3 = -a_1^{*4} f^* g' \Sigma_- - a_1^2 a_1^{*2} f^* g'^* \Sigma_- - a_1^{*4} d^* \Sigma_-^2 - a_1^2 a_1^{*2} f f^* \Sigma_+ - a_1^4 g'^{*2} \Sigma_+ - a_1^2 a_1^{*2} d \Sigma_- \Sigma_+/2 + a_1^{*4} f^* g' S_-/\gamma + a_1^2 a_1^{*2} f^* g'^* S_-/\gamma + 2a_1^{*4} d^* \Sigma_- S_-/\gamma + a_1^2 a_1^{*2} d \Sigma_+ S_-/2\gamma - a_1^{*4} d^* S_-^2/\gamma^2 + a_1^2 a_1^{*2} f f^* S_+/\gamma + a_1^4 g'^{*2} S_+/\gamma + a_1^2 a_1^{*2} d \Sigma_- S_+/2\gamma + a_1^2 a_1^{*2} \gamma \Sigma_- \Sigma_+ S_+ - a_1^2 a_1^{*2} d S_- S_+/2\gamma^2 - a_1^2 a_1^{*2} \Sigma_+ S_- S_+ - a_1^2 a_1^{*2} \Sigma_- S_+^2 + a_1^2 a_1^{*2} S_- S_+^2/\gamma.$$

2.2 Quantum mechanics

Spin operator was defined in Part II either by components in external reference frame (upper index, S^i) or by components in the special coordinate system \vec{e}_i , related with string dynamics (lower index, S_i). The commutation relations:

$$[S^i, S^j] = i\epsilon_{ijk} S^k, \quad [S_i, S_j] = -i\epsilon_{ijk} S_k, \quad [S^i, S_j] = 0$$

correspond to raising/lowering operators

$$S^{\pm} = S^1 \pm iS^2, \quad [S^3, S^{\pm}] = \pm S^{\pm}, \quad [S^+, S^-] = 2S^3, \\ S_{\pm} = S_1 \pm iS_2, \quad [S_3, S_{\pm}] = \mp S_{\pm}, \quad [S_+, S_-] = -2S_3,$$

i.e. S^+ raises S^3 by 1, S^- lowers S^3 by 1; S_+ lowers S_3 by 1, S_- raises S_3 by 1. In further mechanics only low-index operators S_i will participate. In Part II the oscillator variables were composed to the operators $\Sigma_{\pm}, A_3^{(2)}$ with commutation relations $[A_3^{(2)}, \Sigma_{\pm}] = \pm \Sigma_{\pm}$, i.e. Σ_+ raises $A_3^{(2)}$ by 1, Σ_- lowers $A_3^{(2)}$ by 1. These operators define a constraint $\chi_3 = S_3 - A_3^{(2)}$, representing a symmetry of the mechanics, under which the state vectors are invariant: $\chi_3 |\Psi\rangle = 0$. We see that the operators Σ_{\pm} and S_{\pm} have similar commutation relations with χ_3 : $[\chi_3, \Sigma_{\pm}] = \mp \Sigma_{\pm}$, $[\chi_3, S_{\pm}] = \mp S_{\pm}$, so that a linear combination of Σ_+ and S_+ lowers χ_3 by 1, while a linear combination of Σ_- and S_- raises χ_3 by 1. We will also say that Σ_+ and S_+ have χ_3 -charge (-1) , while Σ_- and S_- have χ_3 -charge 1. Similarly the concept of charges, introduced in Part II, can be extended to other operators from oscillator and spin parts of the mechanics.

Matrix elements of spin components do not depend on the representation of the algebra and have well known form [3]:

$$\langle S(S-1)S^3 | S_+ | S S S S^3 \rangle = \sqrt{S(S+1) - S_3(S_3-1)}, \\ \langle S(S+1)S^3 | S_- | S S S S^3 \rangle = \sqrt{S(S+1) - S_3(S_3+1)},$$

all other elements vanish. Concrete representation of quantum top is described by Wigner's functions $\mathcal{D}_{S_3 S_3}^S$ [4, 3]. Here S characterizes the eigenvalue of Casimir operator $S^i S^i = S_i S_i = S(S+1)$, commuting with all spin components. S is integer for single-valued representation of $SO(3)$ and half-integer for double-valued one. In Appendix 2 we show that in our problem only integer values of S should be taken.

Ordering rules. We use the same ordering of elementary operators as defined in Part II, Table 1. In the products of spin components S_{\pm} , commuting with elementary operators, we select the ordering $S_+ S_-$, so that S_3 -raising operator S_- stands on the right and annihilates the states with maximal spin projection $S_3 = S$. We remind that classically $S_3 = S = P^2/2\pi$ corresponds to one-modal solution,

straight line string, associated with the leading Regge trajectory. Quantum analog of (3) is constructed as follows:

$$\alpha_2 = \sum_{n \geq 1} \tilde{n}_1^{-2n+1} : P_n :, \quad (4)$$

where $\tilde{n}_1 = a_1^+ a_1 + c_1$. Here we introduce a constant term c_1 , whose contribution vanishes on classical level (in the limit of large occupation numbers $a_1^+ a_1$), and add analogous terms in quantum definition $\gamma = (L_0^{(2)} + c_2)^{-1/2}$ and in the definition of mass-squared operator, which we fix as follows:

$$\frac{P^2}{2\pi} = L_0^{(2)} + 2\alpha_2 \alpha_2^+ + c_3. \quad (5)$$

Note that this definition differs from one used in Part II for $S = 0$ case. Later we will show that this definition is preferable for the description of arbitrary spin case.

Lemma 5 (*convergence, analog of PII-L7*):

$\langle L_0^{(2)} = N_1, S | : P_n : | L_0^{(2)} = N_2, S \rangle = 0$, if $n > \min\{1 + (N_1 + N_2)/2, (4 + 2(N_1 + N_2) + 4S)/5\}$.

The resulting spectrum $(P^2/2\pi, S)$ is shown on fig.3. The spectrum has common features with the upper part of $(L_0^{(2)}, A_3^{(2)})$ spectrum, shown on fig.2. The beginning of the spectrum $(P^2/2\pi, S)$ consists of three almost linear Regge trajectories. There is a 2-unit gap between the first and the second trajectories. The third trajectory starts at $S = 1$ level. For the next trajectories the degenerate states of fig.2 become splitted on fig.3. The states at $(P^2/2\pi, S) = (3, 1)$ and $(4, 0)$ comprise two numerically close pairs with $P^2/2\pi = 3, 3.0046$ and $P^2/2\pi = 4, 4.0066$, while the other states on fig.3 are non-degenerate (not counting trivial degeneration for the upper-index $S^3 = -S \dots S$ and direction of P_μ). The spectrum is computed for the values $c_1 = 2, c_2 = 4, c_3 = 0$. Smaller values of c_1, c_2 correspond to higher non-linearities in the spectrum, while larger values of c_1, c_2 make the spectrum more linear and closer to the spectrum of $(L_0^{(2)}, A_3^{(2)} \geq 0)$. This behavior is characterized by the following lemmas, where for clarity of statements we fix $c_3 = 0$.

Table 1: eigenvectors with $P^2/2\pi \in \mathbf{Z}$.

$P^2/2\pi = L_0^{(2)}$	$S = S_3 = A_3^{(2)}$	$\{ n_k\rangle\}$
0	0	$ 0\rangle$
2	0	$ 1_1 1_{-1}\rangle$
4	0	$ 2_1 2_{-1}\rangle$
1	1	$ 1_1\rangle$
3	1	$ 1_3\rangle$

Lemma 6 (*analog of PII-L9*): the states from Table 1 are annihilated by α_2^+ and have integer-valued $P^2/2\pi$.

Lemma 7 (*leading term*): let's keep in α_2^+ only the leading $(1/\tilde{n}_1)$ -term: $\alpha_2^+ |_{n=1} = (-\Sigma_- + S_-/\gamma)/\tilde{n}_1$. The states from the first two Regge-trajectories are annihilated by $\alpha_2^+ |_{n=1}$. In this approximation the first two Regge-trajectories have integer-valued $P^2/2\pi$ and are linear: $P^2/2\pi = S + k, k = 0, 2$.

Lemma 8 (*heavy vacuum modes*): in the limit $1 \ll c_1^2 \ll c_2 \ll c_1^4$ the spectrum of $(P^2/2\pi, S)$ tends to the spectrum of $(L_0^{(2)}, A_3^{(2)} \geq 0)$.

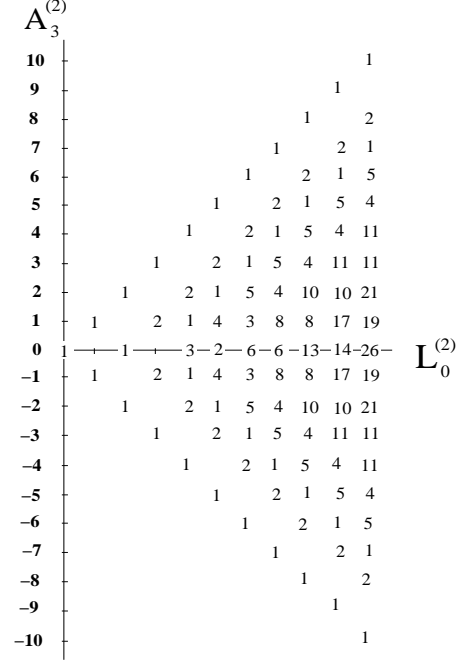


Fig.2. Spectrum $(L_0^{(2)}, A_3^{(2)})$.

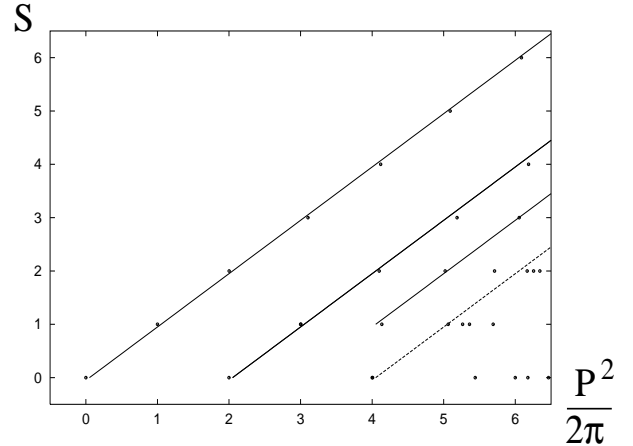


Fig.3. Spectrum $(P^2/2\pi, S)$.

Remark (other ordering rules). We have fixed the ordering $\alpha_2 \alpha_2^+$ in the definition of mass-square operator after testing a number of alternative rules: $a_2^+ a_2, \alpha_2^+ \alpha_2$, etc. The alternative rules produce less regular spectrum $(P^2/2\pi, S)$. Particularly, for the ordering $\alpha_2^+ \alpha_2$ the operator S_+ , present in $\alpha_2 \sim (-\Sigma_+ + S_+/\gamma)$, does not annihilate the states on the leading Regge trajectory $S_3 = S = P^2/2\pi$, and introduces additional non-linearity to this trajectory. For the ordering $a_2^+ a_2$ the operator a_1 , standing on the right in a_2 , annihilates the vacuum state at each S -level: $a_2 |L_0^{(2)} = 0, S\rangle = 0$, therefore $P^2 |L_0^{(2)} = 0, S\rangle = 0$ for any S , the resulting spectrum loses Regge behaviour. In other tested definition we performed a search of the pairs $a_1^+ a_1$ in P_n on the classical level, and later replace them $a_1^+ a_1 \rightarrow \tilde{n}_1$. This definition creates almost linear Regge trajectories for small S , possessing more non-linearity at large S .

Conclusion

In this series of papers we have demonstrated a possibility of construction of the quantum theory of Nambu-Goto string in the space-time of dimension $d = 4$. The general approach is the selection of the light-cone gauge with the gauge axis related in Lorentz-invariant way with the world sheet. In this approach the Lorentz group transforms the world sheet together with the gauge axis and is not followed by reparametrizations. As a result, the theory becomes free of anomalies in Lorentz group and in the group of internal symmetries of the system. The constructed quantum theory possesses spin-mass spectrum with Regge-like behaviour.

Certain problems are still present in this theory, which however do not hinder its implementations, e.g. for the construction of string models of the hadrons. The results, produced by the theory, are influenced by ordering of operators and other details of quantization procedure. The theory does not contain *algebraic anomalies*, but possesses the features, which can be called *spectral anomalies*. Particularly, Hamiltonian $P^2/2\pi$, classically generating 2π -periodic evolution, in quantum theory is influenced by ordering rules and does not have strictly equidistant spectrum. This fact does not create problems for the hadronic models, where this spectrum is subjected to phenomenological corrections and experimentally is not strictly equidistant as well. The theory also possesses a topological defect, appearing as a discrete gauge symmetry, identifying the points in the phase space (Gribov's copies). This classical symmetry is related with discrete non-linear reparametrizations of the world sheet and is not preserved on the quantum level. In our construction we use the expansion series in the vicinity of one Gribov's copy, by these means distinguishing it in the quantum theory. We have also shown that the leading term of the expansion, which has a minimal ordering ambiguity and is easier for computation, is sufficient to reproduce Regge behaviour of the spectrum. Therefore, practically one can keep this term to describe the main effect and include further terms in the form of phenomenological corrections, together with the contributions of other nature [16-21]: gluonic tube thickness, quark masses, charges, spin-orbital interaction, etc.

References

- [1] I. Nikitin, String theory in Lorentz-invariant light cone gauge, hep-th/9906003.
- [2] I. Nikitin, L. Nikitina, String theory in Lorentz-invariant light cone gauge - II, hep-th/0301204.
- [3] L.D. Landau, E.M. Lifshitz, Course of Theoretical Physics, Volume 3, Quantum Mechanics, Non-relativistic, Pergamon, 1977.
- [4] E. Wigner, Group Theory, Academic Press, New York, 1959.
- [5] B.A. Dubrovin, S.P. Novikov, A.T. Fomenko, Modern Geometry, Moscow, Nauka 1979.
- [6] V.I. Arnold, Uspekhi Mat. Nauk 1972. V.27 p.119.
- [7] A. Gray, "Monkey Saddle." Modern Differential Geometry of Curves and Surfaces with Mathematica, 2nd ed. Boca Raton, FL: CRC Press, pp. 299-301, 382-383, and 408, 1997.
- [8] V.I. Arnold, Mathematical methods of classical mechanics, Moscow: Nauka 1979.
- [9] M.S. Plyushchay, G.P. Pron'ko and A.V. Razumov, Baryon String Model. 3. Quantum Theory of One Mode Configurations of Three String, Theor. Math. Phys. 1986. V.67 p.576.

- [10] I.N. Nikitin, Particular types of string motion with anomaly-free quantization, Theor.Math.Phys. 1996. V.109 N2 p.1400.
- [11] M.S. Plyushchay and A.V. Razumov, Dirac versus reduced phase space quantization for systems admitting no gauge conditions, Int. J. Mod. Phys. A 1996. V.11 p.1427.
- [12] V. I. Borodulin, O. L. Zorin, G. P. Pron'ko, A. V. Razumov and L. D. Solov'ev, Single-mode approximation in the quantum theory of a relativistic string. String field. Theor. Math. Phys. 1986. V.65 pp.1050-1065.
- [13] L. Schulman, Phys. Rev. 1968. V.176 N.5 pp.1558-1569.
- [14] H.B.G. Casimir, Rotation of a Rigid Body in Quantum Mechanics, J.B.Wolter's, Groningen, 1931.
- [15] H. Weyl, The theory of groups and quantum mechanics, New York: Dover, 1950.
- [16] Y. Nambu, Phys. Rev. D 1974. V.10 N12 p.4262.
- [17] G.P. Pron'ko, Nucl. Phys. B 1980. V.165 p.269.
- [18] A.A. Migdal, Nucl. Phys. B 1981. V.189 p.253.
- [19] E.V. Gedalin, E.G. Gurvich, Sov. J. Nucl. Phys. 1990. V.52 p.240.
- [20] E.B. Berdnikov, G.G. Nanobashvili, G.P. Pron'ko, The Relativistic Theory for Principal Trajectories and Electromagnetic Transitions of Light Mesons, Int. J. Mod. Phys. A 1993. V.8. N14. p.2447; V.8. N15. p.2551.
- [21] B.M. Barbashov, V.V. Nesterenko, Introduction to the Relativistic String Theory, Singapore, World Scientific, 1990.

Appendix 1: proofs for the lemmas.

1. In the space of variables $M = (\vec{e}_3, \vec{q}_{n\perp}, \vec{p}_{n\perp})$, introduced in Part II, the subgroup generated by χ_3 acts trivially, and the whole gauge group of χ_i -constraints becomes equivalent to $SO(3)/SO(2) \sim S^2$. This group defines the vector fields $\vec{q}_{n\perp}(\vec{e}_3), \vec{p}_{n\perp}(\vec{e}_3)$, tangent to the sphere $|\vec{e}_3| = 1$. Each of these vector fields defines an embedding $f: S^2 \rightarrow TM(S^2)$ of the sphere to its tangent bundle. Let \tilde{G} be an image of this embedding for the vector field $\vec{q}_{s\perp}$. It is a smooth 2-dimensional submanifold of 4-dimensional tangent bundle. The gauge condition $\vec{q}_{s\perp} = 0$ defines another 2-dimensional submanifold \tilde{F} , which can be identified with original sphere S^2 . Due to a theorem [5] p.525, the index of intersection for these manifolds coincides with the index of singular points for the corresponding vector field. Then we trivially lift this construction to the whole space M .

2. The orbits of Gribov's copies are defined as zero level curves of the function $F(\vec{e}_3) = (\vec{q}_n \times \vec{p}_n, \vec{e}_3) \sim i(\vec{a}_n \times \vec{a}_n^*, \vec{e}_3)$. This function does not depend on phase rotations, thus the orbits are not changed after the multiplication by the phase factor. It's easy to verify that in both definitions the evolution $a_n \rightarrow a_n e^{-in\tau}$ is equivalent to the motion of the marked point O along the supporting curve $\vec{Q}(\sigma)$ under the action of uniform shifts: $\sigma \rightarrow \sigma + \tau$. The only difference is that for PII-Eq.(12) these shifts are performed in lcg-parametrization, while (1) corresponds to the natural parametrization.

3. The structure of singularities near the poles has been described in PII-L5,6. On the whole sphere of \vec{e}_3 for the straight string solution $\vec{Q}(\sigma) = (\cos \sigma, \sin \sigma, 0)$ the integral (1) can be evaluated in terms of Bessel functions: $\vec{a}_n = (-i)^n \sqrt{\pi/8} (J_{n+1}(n\rho) e^{i(n+1)\alpha} + J_{n-1}(n\rho) e^{i(n-1)\alpha}, -iJ_{n+1}(n\rho) e^{i(n+1)\alpha} + iJ_{n-1}(n\rho) e^{i(n-1)\alpha}, 0)$, where $\vec{e}_3 =$

$(\rho \cos \alpha, \rho \sin \alpha, \rho_z)$, $0 \leq \rho \leq 1$, $\rho^2 + \rho_z^2 = 1$, $n = 1, 2, \dots$. The real part $\vec{q}_n = \text{Re}(\vec{a}_n) = \sqrt{\pi/8}(J_{n+1}(n\rho) \cos \phi_+ + J_{n-1}(n\rho) \cos \phi_-, J_{n+1}(n\rho) \sin \phi_+ - J_{n-1}(n\rho) \sin \phi_-, 0)$, where $\phi_{\pm} = (n \pm 1)\alpha - \pi n/2$. Zeros of $\vec{q}_{n\perp} = \vec{q}_n - (\vec{q}_n \cdot \vec{e}_3)\vec{e}_3$ correspond to $\vec{q}_n \times \vec{e}_3 = (q_n^2 e_3^3, -q_n^1 e_3^3, q_n^1 e_3^2 - q_n^2 e_3^1) = 0$. The solutions disjoin to the following branches:

- (b1) $e_3^3 = 0$, equator: $q_n^1 e_3^2 - q_n^2 e_3^1 = 0$;
- (b2) $e_3^3 \neq 0$, $q_n^1 = q_n^2 = 0$.

For the case (b1) $\rho = 1$ and after simplifications we have $(J_{n-1}(n) - J_{n+1}(n)) \cdot \sin(n\alpha - \pi n/2) = 0$, i.e. $\alpha = \pi/2 + \pi k/n$, $k = 0 \dots 2n - 1$. Considering the expansion of the vector field e.g. near the point $\alpha = \pi/2$ in the local coordinates $(\Delta\alpha, \rho_z)$, we have $q_{n\perp} \sim (-n(J_{n-1}(n) - J_{n+1}(n))\Delta\alpha, -(J_{n-1}(n) + J_{n+1}(n))\rho_z)$. Because of the property $J_{n-1}(n) > J_{n+1}(n) > 0$ (see below) we conclude that this singular point is the node. For the vector fields, corresponding to the straight line string, the evolution is equivalent to the rotation about z-axis. The evolution during $\Delta\tau_n = \pi/n$ matches the node on the equator to the neighbour one. Let's consider small perturbations of the string from the straight configuration. Non-degenerate points persist and preserve their type after the deformation. From PII-L3 we know that singular points move along zero-level curves of the function $F(\vec{e}_3) = (\vec{q}_n \times \vec{p}_n, \vec{e}_3)$. For the straight line string this function is

$$F \sim i \begin{vmatrix} \rho \cos \alpha & \rho \sin \alpha & \rho_z \\ a_n^1 & a_n^2 & 0 \\ a_n^{1*} & a_n^{2*} & 0 \end{vmatrix} \sim \rho_z (J_{n-1}^2(n\rho) - J_{n+1}^2(n\rho)).$$

Near the equator $F \sim \rho_z$, i.e. the equator is non-degenerate zero level curve of this function: $\partial F / \partial \rho_z \neq 0$. Parameterizing zero level curve by the longitude: $\vec{e}_3(\alpha)$, after small deformations: $F(\vec{e}_3 + \delta\vec{e}_3) + \delta F(\vec{e}_3) = 0$, for the shifts of the latitude we have: $\delta\rho_z = -(\partial F / \partial \rho_z)^{-1} \delta F$. Therefore, the curve will be slightly deformed in the vicinity of the equator. It was proven in the Part II, that the vector field reverses its sign after the lapse of time $\Delta\tau_n$. During this time the pattern of singularities returns to the initial state. Thus, the nodes near the equator should move to the neighbor ones, to satisfy the continuous limit with the straight string configuration.

For the case (b2) $\rho < 1$ and we have a system

$$\begin{cases} J_{n-1}(n\rho) \sin(\phi_+ + \phi_-) = 0, \\ J_{n+1}(n\rho) + J_{n-1}(n\rho) \cos(\phi_+ + \phi_-) = 0. \end{cases}$$

Here we again have two branches:

- (b21) $J_{n+1}(n\rho) = J_{n-1}(n\rho) = 0$;
- (b22) $\phi_+ + \phi_- = \pi k$, $J_{n+1}(n\rho) + (-)^k J_{n-1}(n\rho) = 0$.

In the case (b21) we have only solution $\rho = 0$ at $n > 1$. It gives pole singularities described in PII-L5.6. Near this solution $J_{n+1} \ll J_{n-1} \ll 1$ and in the passage around this point the vector $(q_n^1, q_n^2) \sim \rho^{n-1}(\cos \phi_-, -\sin \phi_-)$ performs $(n-1)$ revolutions in the direction opposite to the passage. It corresponds to the saddle for $n = 2$ and multi-saddle for $n > 2$. In the complex plane of $z = \rho e^{i\alpha}$ the mapping $z \rightarrow q = q_n^1 + i q_n^2$ near this point can be represented as $q \sim (z^*)^{n-1}$. Considering small deformations of the string from straight configuration, we introduce a correction $(z^*)^{n-1} + \delta q$, where $\delta q(z, z^*) = \delta q_0 + \delta q_0 z z^* + \delta q_0 z^* z^* + \dots$ is small together with its derivatives, and in small vicinity of the singular point we keep only the constant term δq_0 . At a given point there is 1-1 correspondence between the set $(q_n, p_n)_0$ and the shape of supporting curve, and the arbitrary small variations δq_0 can be reproduced by variations

of supporting curve. That's why we can apply the same perturbation analysis as for general vector fields, in spite of the fact that we consider the fields of special form. New singular points are $z_k = (-\delta q_0^*)^{1/(n-1)} e^{2\pi i k/(n-1)}$, $k = 0 \dots n-2$. Expansion of the field in their vicinity has a form $q = (z_k^* + \Delta z^*)^{n-1} + \delta q_0 \sim (n-1)(z_k^*)^{n-2} \Delta z^*$, therefore we have $(n-1)$ saddles. Considering their evolution: $q \rightarrow q \cos n\tau + p \sin n\tau$, where $p \sim i(z^*)^{n-1} + \delta p$, we have $(z^*)^{n-1} e^{in\tau} + \delta q \cos n\tau + \delta p \sin n\tau = 0$, i.e. $z_k = (-\delta z_1^* - \delta z_2^* e^{2in\tau})^{1/(n-1)} e^{2\pi i k/(n-1)}$, where $\delta z_1 = (\delta q - i\delta p)/2$, $\delta z_2 = (\delta q + i\delta p)/2$. If $n = 2$, we have a single saddle moving along a closed loop with a period $\Delta\tau_2 = \pi/2$, as described in PII-L6. If $n > 2$, the dynamics is more complex, see fig.4. Particularly, if $\delta z_1 = 0$, $\delta z_2 \neq 0$, $n-1$ saddles move along a common circle, matching the neighbour one after the lapse of time $\Delta\tau_n = \pi/n$. If $\delta z_1 \neq 0$, $\delta z_2 = 0$, the saddles stay fixed. Generally, if $0 < |\delta z_2| < |\delta z_1| \ll 1$, the origin $z = 0$ is placed outside the circle $\delta z_1 + \delta z_2 e^{-2in\tau}$, and the complex root of $(n-1)$ -th order gives $(n-1)$ saddles moving along disjoint loops with a period $\Delta\tau_n$. If $0 < |\delta z_1| < |\delta z_2| \ll 1$, the origin is inside the circle and the saddles move along a common loop. The separatrix $|\delta z_1| = |\delta z_2|$ for $n > 3$ is structurally unstable and under the influence of higher order corrections is unfolded to further complex cases.

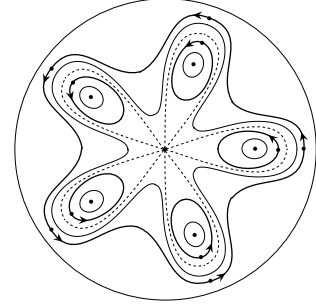


Fig.4. Unfolding of multi-saddle, $n = 6$.

Note: this phenomenon resembles the bifurcation of degenerate critical point of the function $f = x^3 - 3xy^2$ [6] (known also as “monkey saddle” [7]), and the structure of phase flows near high order resonances of Hamiltonian systems [8].

In the case (b22) we have $\alpha = \pi k/2n$, $k = 0 \dots 4n - 1$, $J_{n+1}(n\rho) - J_{n-1}(n\rho) = 0$ for odd k and $J_{n+1}(n\rho) + J_{n-1}(n\rho) = 0$ for even k . The solution $\rho = 0$, $n > 1$ has been already considered. There are no solutions in the interval $0 < \rho \leq 1$ due to the inequality $J_{n-1}(n\rho) > J_{n+1}(n\rho) > 0$, which follows from easily provable relation for Bessel functions: $J_{n-1}(x) > J_n(x) > J_{n+1}(x) > \dots > 0$ for $0 < x \leq n$, $n = 1, 2, 3, \dots$

4. The equations (6) of Part II in the arbitrary spin case can be rewritten as

$$\begin{aligned} a_2 &= \frac{a_1^2}{n_1^2} \cdot \left(-z + \frac{S_+}{\gamma} (1 + \beta) \right), \\ a_2^* &= \frac{a_1^{*2}}{n_1^{*2}} \cdot \left(-z^* + \frac{S_-}{\gamma} (1 + \beta) \right), \\ \beta &= a_2^* a_2 \gamma^2 - \beta^2 / 2, \end{aligned} \quad (6)$$

where $n_1 = a_1^* a_1$, $z = \Sigma_+ + f^* a_2^* + g'^* a_2 + d^* a_2^{*2} + da_2 a_2^* / 2$, $(1 + \beta) / \gamma = \sqrt{P^2 / 2\pi}$. Substituting the expansions

$$a_2 = \sum_{n \geq 1} \frac{P_n a_1^2}{n_1^{2n}}, \quad \beta = \sum_{n \geq 1} \frac{b_n}{n_1^{2n}},$$

we obtain the following recurrent relations:

$$\begin{aligned}
P_1 &= -\Sigma_+ + \frac{S_+}{\gamma}, \quad b_1 = 0, \\
P_n &= -f^* a_1^{*2} P_{n-1}^* - g'^* a_1^2 P_{n-1} - d^* a_1^{*4} \sum_{1 \leq m \leq n-2} P_{n-m-1}^* P_m^* \\
&\quad - \frac{1}{2} d a_1^{*2} a_1^2 \sum_{1 \leq m \leq n-2} P_{n-m-1} P_m^* + \frac{S_+}{\gamma} b_{n-1}, \quad n > 1, \\
b_n &= a_1^{*2} a_1^2 \gamma^2 \sum_{1 \leq m \leq n-1} P_{n-m}^* P_m - \frac{1}{2} \sum_{1 \leq m \leq n-1} b_{n-m} b_m, \quad n > 1.
\end{aligned}$$

Then the properties (i)-(v) can be easily proven by induction. The property (i) also follows from the scaling symmetry of the system (6): formal transformations $\{n_1 \rightarrow \sqrt{C} \cdot n_1, v \rightarrow C \cdot v, v \in (d, f, g', \Sigma_-, S_- \text{ and their conjugates})\}$ and $\{n_1 \rightarrow C \cdot n_1, a_1 \rightarrow C \cdot a_1\}$ preserve a_2, β ; the property (iii) follows from reflection symmetry: $a_1 \rightarrow -a_1$ preserves a_2, β . The property (ii) follows from the fact that $a_2 = \beta = 0$ is the solution of (6) at $\Sigma_{\pm} = S_{\pm}$.

5. Let's consider a monomial of P_n , substitute the definitions of elementary operators $d = d_+ - d_-$, $f = f_+ - f_-$, $g' = g'_- - g_+$ (see PII-Eq.(7)), expand it to a number of (secondary) monomials and normally order each one. Let $n(d_{\uparrow}), n(f_{\uparrow}), n(g_{\uparrow}), n(a_{1\uparrow})$ be the numbers of $L_0^{(2)}$ -raising operators in the secondary monomial, $n(d_{\downarrow}), n(f_{\downarrow}), n(g_{\downarrow}), n(a_{1\downarrow})$ be the numbers of $L_0^{(2)}$ -lowering operators. Using the definitions of the charges (Table 1 in Part II), we see that the secondary monomial is represented as a diagonal with offsets $\Delta_{\uparrow} L_0^{(2)} = 4n(d_{\uparrow}) + 2n(f_{\uparrow}) + 2n(g'_{\uparrow}) + n(a_{1\uparrow})$, $\Delta_{\downarrow} L_0^{(2)} = 4n(d_{\downarrow}) + 2n(f_{\downarrow}) + 2n(g'_{\downarrow}) + n(a_{1\downarrow})$ in the matrix, displayed at fig.5a: $\langle L_0^{(2)} = N_1 | \text{mon} | L_0^{(2)} = N_2 \rangle \sim \langle L_0^{(2)} = N_1 - \Delta_{\uparrow} L_0^{(2)} | \text{diag} | L_0^{(2)} = N_2 - \Delta_{\downarrow} L_0^{(2)} \rangle$. Here *diag* represents $L_0^{(2)}$ -neutral part of the monomial, consisting of the operators $\Sigma_{\pm}, S_{\pm}, \gamma$, and non-zero value of this matrix element corresponds to $N_1 - \Delta_{\uparrow} L_0^{(2)} = N_2 - \Delta_{\downarrow} L_0^{(2)} \geq 0$.

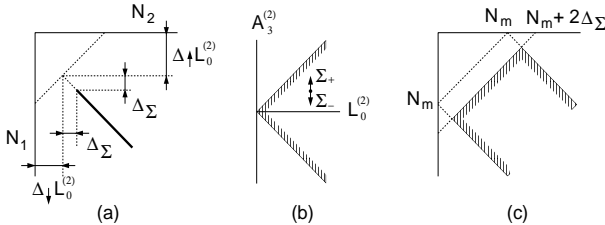


Fig.5. To the proof of lemma 5.

Then, using the inequality $|A_3^{(2)}| \leq L_0^{(2)}$ and charge properties of Σ_{\pm} , see fig.5b, we conclude that non-zero value for the considered matrix element corresponds to the following restrictions on the number of Σ_{\pm} -operators: $n(\Sigma_+) \leq 2(N_2 - \Delta_{\downarrow} L_0^{(2)})$, $n(\Sigma_-) \leq 2(N_2 - \Delta_{\downarrow} L_0^{(2)})$, i.e. $N_2 \geq \Delta_{\downarrow} L_0^{(2)} + \Delta_{\Sigma}$, $\Delta_{\Sigma} = \max(n(\Sigma_+), n(\Sigma_-))/2$. As a result, non-zero entries in the diagonal, shown on fig.5a, receive an additional offset. After summation over all secondary monomials non-zero entries of the matrix are localized in the region, shown on fig.5c. Here $N_m = \Delta_{\uparrow} L_0^{(2)} + \Delta_{\downarrow} L_0^{(2)} = 4n(d) + 2n(f) + 2n(g) + n(a_1)$ and $n(x)$ represents the number of variables (x, x^*) in the primary monomial. Particularly, non-zero entries are localized at $N_1 + N_2 \geq N_m + 2\Delta_{\Sigma}$. For the number of S_{\pm} -operators we have the following restrictions: $n(S_+) \leq 2S$,

$n(S_-) \leq 2S$. Then, using the property (i) from the structural lemma: $n(S_{\pm}, \Sigma_{\pm}, d, f, g) = n$, $n(a_1) = 2(n-1)$, we construct the following system of 11 linear inequalities and 1 linear equation:

$$\begin{aligned}
4n(d) + 2n(f) + 2n(g) + n(\Sigma_+) &\leq N_1 + N_2 + 2 - 2n, \\
4n(d) + 2n(f) + 2n(g) + n(\Sigma_-) &\leq N_1 + N_2 + 2 - 2n, \\
0 \leq n(S_+) \leq 2S, \quad 0 \leq n(S_-) \leq 2S, \\
n(\Sigma_+) \geq 0, \quad n(\Sigma_-) \geq 0, \quad n(d) \geq 0, \quad n(f) \geq 0, \quad n(g) \geq 0, \\
n(d) + n(f) + n(g) + n(\Sigma_+) + n(\Sigma_-) + n(S_+) + n(S_-) &= n.
\end{aligned}$$

The inequalities define a convex polyhedron in 9-dimensional space $(n, N_1 + N_2 + 2, S, n(d), n(f) + n(g), n(\Sigma_+), n(\Sigma_-), n(S_+), n(S_-))$. The linear equation defines its 8-dimensional slice. Projecting it to a 3-dimensional subspace of parameters $(n, N_1 + N_2 + 2, S)$, we obtain a convex polyhedron, which represents the region of existence of the solutions. Solving the system by *Mathematica*, we have $n \leq \min\{1 + (N_1 + N_2)/2, (4 + 2(N_1 + N_2) + 4S)/5\}$. This condition defines a region, where non-zero entries of the matrix element considered in the lemma are located.

6. The states, annihilated by α_2^+ , have $P^2/2\pi = L_0^{(2)} \in \mathbf{Z}$, at $c_3 = 0$. Due to the property (ii) of structural lemma each monomial in P_n contains at least one operator from the group (Σ_{\pm}, S_{\pm}) . After the normal ordering some number of $L_0^{(2)}$ -lowering operators can also appear on the right of Σ_{\pm} . Due to the charge properties and the property (iii) of lemma 4, the $L_0^{(2)}$ -lowering operators together decrease $L_0^{(2)} \rightarrow L_0^{(2)} - 2k$, $k \in \mathbf{Z}$, $k \geq 1$. The vacuum state $(P^2/2\pi, S) = (L_0^{(2)}, A_3^{(2)}) = (0, 0)$ is annihilated by all these operators. The state $(P^2/2\pi, S) = (L_0^{(2)}, A_3^{(2)}) = (1, 1)$ is annihilated by Σ_{\pm} -operators, together with other states on the leading Regge trajectory, see fig.2. If there are any $L_0^{(2)}$ -lowering operators at the right, they decrease $L_0^{(2)}$ by ≥ 2 and annihilate this state. It is also annihilated by S_- and generally is not annihilated by S_+ . However, due to the property (iv) in lemma 4 each S_+ enters to α_2^+ together with a_1^2 , which annihilates this state. For the state $(P^2/2\pi, S) = (L_0^{(2)}, A_3^{(2)}) = (2, 0)$ the terms with S_{\pm} are inactive. Σ_{\pm} annihilate this state, see fig.2. If there are any $L_0^{(2)}$ -lowering operators at the right, they can transform this state only to vacuum, and the vacuum is also annihilated by Σ_{\pm} . Similarly, on the states $(P^2/2\pi, S) = (L_0^{(2)}, A_3^{(2)}) = (4, 0)$ the terms with S_{\pm} are inactive. There are 3 states on the level $(L_0^{(2)}, A_3^{(2)}) = (4, 0)$, 1 state on the level $(L_0^{(2)}, A_3^{(2)}) = (4, 1)$ and 1 state on the level $(L_0^{(2)}, A_3^{(2)}) = (4, -1)$, see fig.2. As a result, the operator Σ_+ annihilates 2-dimensional subspace of $(L_0^{(2)}, A_3^{(2)}) = (4, 0)$ and one state in this subspace is also annihilated by Σ_- . Using the definition of Σ_{\pm} , it's easy to verify that $\Sigma_{\pm} |2_1 2_{-1}\rangle = 0$. If there are any $L_0^{(2)}$ -lowering operators at the right of Σ_{\pm} , they can transform this state to the states with $L_0^{(2)} = 0, 2$, which are also annihilated by Σ_{\pm} , see fig.2. There are 2 states on the level $(L_0^{(2)}, A_3^{(2)}) = (3, 1)$: $|1_3\rangle, |2_1 1_{-1}\rangle$. Both states are annihilated by Σ_{\pm} . If there are any $L_0^{(2)}$ -lowering operators at the right, they transform these states to $L_0^{(2)} = 1$, also annihilated by Σ_{\pm} . Both states are annihilated by S_- . Generally they are not annihilated by S_+ , and due to the property (iv) in lemma 4 each S_+ enters to α_2^+ together with a_1^2 , which annihilates one of these states: $|1_3\rangle$.

7. In $\alpha_2^+|_{n=1} = (-\Sigma_- + S_-/\gamma)/\tilde{n}_1$ the operator Σ_- decreases $A_3^{(2)}$ by 1, the operator S_- increases S_3 by 1. Let's consider the states $A_3^{(2)} = S_3 = S \geq 0$, annihilated by S_- . On fig.2 we see that Σ_- annihilates the leading Regge trajectory, because there are no states immediately below this trajectory. Concerning the second trajectory $0 \leq A_3^{(2)} = L_0^{(2)} - 2$, one state at $(L_0^{(2)}, A_3^{(2)}) = (2, 0)$ and two states at $(L_0^{(2)}, A_3^{(2)}) = (3, 1)$ are annihilated by Σ_- due to the same reason, while the sequence of double states $2 \leq A_3^{(2)} = L_0^{(2)} - 2$ is transformed by the operator Σ_- to the sequence of non-degenerate states $1 \leq A_3^{(2)} = L_0^{(2)} - 3$, thus annihilating one state from each pair. As a result, the described states are annihilated by $\alpha_2^+|_{n=1}$ and in the considering approximation these states have $P^2/2\pi = L_0^{(2)}$, from here we obtain the statement of the lemma.

8. $\alpha_2^+ = \sum P_n^+/\tilde{n}_1^{2n-1}$, where $P_n = O(\gamma^{-(n+1)/2})$ due to the property (v) of lemma 4. Using the definitions $\tilde{n}_1 = a_1^+ a_1 + c_1$, $\gamma = (L_0^{(2)} + c_2)^{-1/2}$, in the limit $1 \ll c_1^2 \ll c_2 \ll c_1^4$ we have $\alpha_2^+|_n \sim c_2^{[(n+1)/2]/2}/c_1^{2n-1}$, i.e. $\alpha_2^+|_{n=1} \sim c_2^{1/2}/c_1 \gg 1$, $\alpha_2^+|_{n=2} \sim c_2^{1/2}/c_1^3 \ll 1/c_1 \ll 1$, $\alpha_2^+|_{n \geq 3} \sim c_2^{[(n+1)/2]/2}/c_1^{2n-1} \leq c_2^{(n+1)/4}/c_1^{2n-1} \ll 1/c_1^{n-2} \ll 1$. Writing explicitly the leading contribution: $\alpha_2^+ = S_- \cdot c_2^{1/2}/c_1 + o(1)$, we see that the states with $S = S_3 = A_3^{(2)}$ are annihilated by α_2^+ in the described approximation, while other states receive large contribution to $P^2/2\pi$ and are shifted away from the origin of the spectrum. Due to this property, the spectrum of $(P^2/2\pi, S)$ tends to the spectrum of $(L_0^{(2)}, A_3^{(2)} \geq 0)$, provided that $c_3 = 0$.

Appendix 2: super-selection rule.

In several earlier works the quantum top appeared in the context of relativistic string dynamics. Particularly, the paper [9] describes a special family of motions in a theory of Y-shaped strings, globally isomorphic to the phase space of the top $\mathbf{R}^3 \times SO(3)$. In the paper [10] a similar family was selected in the phase space of open strings. In the present paper we also have $SO(3)$ -factor in the topology of the phase space. As a manifold, it has a fundamental group $\pi_1(SO(3)) = \mathbf{Z}_2$, i.e. it possesses two homotopically non-equivalent classes of contours. The contour, representing one complete revolution, cannot be contracted to a point (unit of the group), while two revolutions are contractible [14]. This fact gives a possibility to construct ray representations of rotation group, corresponding to integer and half-integer values of spin [15]. The existence of half-integer spin and associated double-valued representations of $SO(3)$ is also explained in terms of path integration technique: non-homotopic contours can contribute to path integrals with different phase factors [13, 9].

The question on the availability of half-integer spin is subtle and requires special consideration in each particular problem. Now we will consider a model example, representing the main features of our problem: the mechanics of 3 particles in 3-dimensional space, $(\vec{x}_n, \vec{p}_n) \in \mathbf{R}^9 \times \mathbf{R}^9$. Let's apply the following canonical transformations: $\Omega = d\vec{p}_n \wedge d\vec{x}_n = d\vec{P} \wedge d\vec{X} + \frac{1}{2}d(\vec{S} \times \vec{e}_i) \wedge d\vec{e}_i + d\rho_{ni} \wedge dq_{ni}$, where $\vec{X} = \sum m_n \vec{x}_n / \sum m_n$, m_n are masses of the particles, $\vec{P} = \sum \vec{p}_n$, $\vec{q}_n = \vec{x}_n - \vec{X}$, $\vec{\rho}_n = \vec{p}_n - m_n/m_3 \cdot \vec{p}_3$, $\vec{S} = \sum \vec{q}_n \times \vec{p}_n = \sum \vec{q}_n \times \vec{\rho}_n$, \vec{e}_i is an orthonormal basis, $\rho_{ni} = \vec{\rho}_n \cdot \vec{e}_i$, $q_{ni} = \vec{q}_n \cdot \vec{e}_i$, and everywhere the sum over repeated indices is assumed. Let's fix the basis with respect

to the particles. The following cases should be considered:

(s₁) \vec{q}_1 and \vec{q}_2 are linearly independent. In this case we can select e.g. $\vec{e}_1 \uparrow \vec{q}_1$, $\vec{e}_2 \uparrow \vec{q}_{2\perp} = \vec{q}_2 - (\vec{q}_2 \vec{q}_1)/\vec{q}_1^2 \cdot \vec{q}_1$. The last term in the symplectic form can be written as $d\rho_{11} \wedge dq_{11} + d\rho_{21} \wedge dq_{21} + d\rho_{22} \wedge dq_{22}$. Here $q_{11} > 0$, $q_{22} > 0$. The obtained phase space has topology $(\mathbf{R}^3) \times (\mathbf{R}^6 \times SO(3))$, where the first factor represents spin-momentum space, the second factor is configuration space, $SO(3)$ is the configuration space of the top.

(s₂) $\vec{q}_1 \neq 0$, $\vec{q}_2 \neq 0$, $\vec{q}_1 \uparrow \vec{q}_2$. Let's direct $\vec{e}_1 \uparrow \vec{q}_1$. The symplectic form can be written as $\Omega = d\vec{P} \wedge d\vec{X} + d(\vec{S} \times \vec{e}_1) \wedge d\vec{e}_1 + d\rho_{11} \wedge dq_{11} + d\rho_{21} \wedge dq_{21}$. Here $\vec{S} \vec{e}_1 = 0$, $q_{11} > 0$, $q_{21} > 0$. The topology of the phase space is $\mathbf{R}^{10} \times TM(S^2)$, the configuration space is $\mathbf{R}^3 \times S^2$. Here the tangent bundle $TM(S^2)$ represents the phase space of rotator.

(s₃) $\vec{q}_1 \neq 0$, $\vec{q}_2 \neq 0$, $\vec{q}_1 \uparrow \downarrow \vec{q}_2$. Corresponds to the same mechanics as (s₂), but $q_{21} < 0$.

(s₄) $\vec{q}_1 \neq 0$, $\vec{q}_2 = 0$. The same mechanics as (s₂), but $q_{21} = 0$ and ρ_{21} omitted: phase space $\mathbf{R}^8 \times TM(S^2)$, configuration space $\mathbf{R}^4 \times S^2$.

(s₅) $\vec{q}_1 = 0$, $\vec{q}_2 \neq 0$. The same mechanics as (s₄), but $q_{22} = 0$ and ρ_{22} omitted.

(s₆) $\vec{q}_1 = \vec{q}_2 = 0$. In this case $\vec{S} = 0$ and $\Omega = d\vec{P} \wedge d\vec{X}$. The phase space is $\mathbf{R}^3 \times \mathbf{R}^3$, scalar particle.

The archetypes (top, rotator, scalar) are essentially the same as described in Sec.2 of Ref.[13]. The important difference is that in our example they appear not as isolated cases, but as a stratification of the configuration space: $\mathbf{R}^6(\vec{q}_1, \vec{q}_2) = \cup_{i=1}^6 s_i$. The strata s_{2-6} have zero measure and $\text{codim}(s_{2,3}) = 2$, $\text{codim}(s_{4,5}) = 3$, $\text{codim}(s_6) = 6$ in \mathbf{R}^6 . The exclusion of these zero measure subsets changes the topological structure of configuration space. Note that the original configuration space is simply connected and quantization of the problem in original representation gives only integer values of spin. All closed loops in the original configuration space are contractible. The contours in this space can be related by a homotopy, intersecting the strata s_{2-6} , as a result, all the contours should contribute to path integrals with the same phase factors. Therefore, only single-valued representation of $SO(3)$ can be used. We conclude that half-integer spin in the considered model example appears as an artefact of the representation and should be rejected.

In our problem constraint $S_3 = A_3 \in \mathbf{Z}$ selects only integer S , however, with formal modifications $A_3 \rightarrow A_3 + 1/2$, classically vanishing after the recovery of Planck's constant, it's possible to introduce half-integer spin to the theory. The above argumentation favors against it. During our construction we reject zero measure subsets of singular cases (see Part II). The original configuration space of open string theory is simply connected, all contours in it are homotopic to each other. Therefore we should not introduce half-integer spin in this theory.

In the problems [9, 10] submanifold $\mathbf{R}^3 \times SO(3)$, representing particular type of string motion, was selected in the original phase space, representing all possible motions. The original configuration space possessed trivial topology: $x_\mu(\sigma) \in C^\infty[0, \pi]$ for open string and $x_\mu^i(\sigma) \in C^\infty[0, \pi]$ with $x_\mu^1(\pi) = x_\mu^2(\pi) = x_\mu^3(\pi)$ for Y-shaped string. Therefore, half-integer spin representations have right to exist in frames of the restricted models [9, 10], but would disappear in full quantum theories.

Appendix 3: Gribov's copies in quantum mechanics.

The Gribov's copies of string theory can be separated to those which belong to the same χ_0 -orbit and are transformed one to the other by the quarter period of the evolution, and

those which belong to different orbits. The factorization of the phase space with respect to χ_0 -transformation identifies the copies on the same χ_0 -orbit.

The discrete symmetry $D_4 = \exp[-i(\pi/2)L_0^{(2)}]$, mapping the Gribov's copies on the χ_0 -orbit one to the other, is associated with the quantum number $Q = L_0^{(2)} \bmod 4$. In the whole phase space, containing the external variables (X, P) , χ_0 -orbit is not closed, but is periodically repeated as $X \rightarrow X + 2Pn$, $n \in \mathbf{Z}$. Considering the evolution in this space, the generator of discrete symmetry should be extended to $D'_4 = \exp[i(\pi/2)(P^2/2\pi - L_0^{(2)})]$. Classically, for the Gribov's copies near the poles this evolution coincides with $D''_4 = \exp[i(\pi/2)\chi_0]$. Indeed, the evolutions D'_4 and D''_4 connect the same Gribov's copies, but along different trajectories, particularly, D'_4 does not contain S_{\pm} -variables, influencing the direction of gauge axis, and D''_4 does. For the Gribov's copies near the equator the evolutions D'_4 and D''_4 connect not the same, but neighbor copies. These formal differences become crucial in quantum mechanics, where $L_0^{(2)}$ has integer-valued spectrum and $M^2/2\pi = L_0^{(2)} + 2\alpha_2\alpha_2^+$ has not. Note that the number Q is associated with $L_0^{(2)}$ and D_4 -symmetry, defined in the phase space of internal variables, independent of (X, P) .

Let's write $\chi_0 = (P^2 - M^2)/2\pi$, where M^2 is a function of the internal variables and has a discrete spectrum. Let's consider the Hamiltonians of interaction H_{int} , which generate transitions in this spectrum. Generally H_{int} should not commute with χ_0 : this would mean that H_{int} is constant on χ_0 -orbit. Also it should not commute with D'_4 , otherwise it would have the periodic properties, which select too narrow class of Hamiltonians. It was shown in paper [20] that not Hamiltonian itself enters to the physical vertex operators, but its average over a period of evolution. This averaging actually inserts a projector onto the subspace $\chi_0 = 0$. In a similar way we can construct an operator J , commuting with χ_0 or D'_4 . Let's consider two cases:

(Ja) J does not contain X . In this case $[J, \chi_0] = 0$ implies $[J, M^2] = 0$, i.e. J cannot create transitions between the states with different masses. Also, $[J, D'_4] = 0$ implies $[J, D_4] = 0$, i.e. J cannot create transitions between the states with different Q .

(Jb) J contains X . In this case the operator with $[J, \chi_0] = 0$ generates simultaneous changes of P^2 and M^2 , preserving the mass shell condition. In a similar way, J creates transitions between Q -sectors, even if the condition $[J, D'_4] = 0$ is satisfied.

Note that the operator M^2 itself belongs to the class (Ja), as a result, it is diagonal with respect to the quantum number Q . The vertex operators generally belong to the class (Jb): they contain X -terms, responsible for the change of P^2 . E.g. the interaction with a planar wave [20] has a factor e^{ikX} , changing $P \rightarrow P - k$. For such interactions Q -sectors are mixed up, therefore no selection rule for Q is necessary.

After factorization of χ_0 -transformations the remaining discrete gauge symmetry is related with the choice between different χ_0 -orbits. For nearly straight string they are represented by equivalent solutions in the vicinity of the northern pole, the equator, and the southern pole. In the obtained spin-mass spectrum the first Regge trajectory corresponds to the northern pole solution, further trajectories are created by expansion (2) in the vicinity of the northern pole solution. Classically there are gauge equivalent solutions near the southern pole and the equator, which possess the same (P^2, S) . In quantum mechanics we do not see these additional solutions in the spectrum. Particularly, the first

Regge trajectory is non-degenerate. We conclude, that the equivalence between these solutions is lost in quantum mechanics. The spectra for additional solutions can be shifted to the region of large masses, or the quantum expansions (4) can even diverge on these solutions. Indeed, the classical solutions in the vicinity of the northern pole possess large n_1 and small n_k , $k \in \mathbf{Z}/\{0, 1, \pm 2\}$, providing the convergence for $(1/n_1)$ -expansion (2). In quantum mechanics the convergence of expansion (4) is supported by the normal ordering of operators and the finite number of occupied modes in $(L_0^{(2)} \leq N)$ -spaces. For the solutions near the southern pole $n_1 \rightarrow 0$, and the usage of $(1/n_1)$ -expansions is problematic. One can use $(1/n_{-1})$ -series to construct a definition of mass shell condition, alternative to (5), however these definitions will substantially differ on the quantum level and in fact will create two distinct theories. For the solutions on the equator infinite number of oscillator modes are excited, and for these solutions the convergence of the expansions is not guaranteed neither on classical nor on quantum level. This argumentation explains why the usage of $(1/n_1)$ -series in the vicinity of the northern pole solution preserves only one Gribov's copy in the quantum theory.

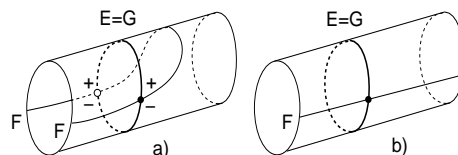


Fig. 6. Example: Gribov's copies in the phase space of planar rotator.

Remark. The problem of Gribov's copies in full generality was addressed in the paper [11]. This paper has considered several systems, possessing the Gribov's copies, and discussed various approaches to their quantization. In the simplest example, planar rotator, the phase space $M = S^1 \times \mathbf{R}$ is formed by a periodical coordinate $\varphi \bmod 2\pi$ and spin variable $S \in \mathbf{R}$. There is a constraint $E = S^1$ of a form $S = \text{Const}$, whose gauge group $G = S^1$ identifies all points on the circle and therefore eliminates from the theory all degrees of freedom. According to [11], such system does not allow gauge fixing condition F of the form $f = 0$, where f is a smooth real-valued function, *globally defined* on M , which has only non-degenerate zeros. Indeed, non-degenerate zero of f divides the circle to the parts with $f > 0$ and $f < 0$, and there is at least one other point with $f = 0$ on the circle, see fig.6a. However, for construction of the reduced phase space it is not necessary for f to be globally defined. For the computation of Dirac's brackets it's only needed that f has been defined locally, in the vicinity of the intersection $E \cap F$. Generally F can be an arbitrary smooth submanifold of M , not necessary representable as zero level of a globally defined function, see fig.6b. Moreover, for the technique [8, 12] only the intersection $E \cap F$ should be specified and the symplectic form of M can be reduced directly to $E \cap F$. In the considered example such class of gauge fixing conditions allows unique intersection between E and F . In this low-dimensional example the surface of constraint E coincides with the orbit of gauge group G , generally they differ. In certain cases the topology of gauge orbit G and gauge fixing condition can lead to multiple intersections. Particularly, if both are closed submanifolds of Euclidean space (with $\dim(G) = \text{codim}(F)$), their intersection index equals zero, giving an even number of transversal intersections [5]. The same property holds if one is a closed submanifold and

the other one is a linear subspace. The set $E \cap F$ can be connected (otherwise the connected component can be taken), and the orbits G of gauge group, to which E is foliated, can intersect F several times. In this case the mechanics possesses Gribov's copies and associated discrete gauge symmetries.

Appendix 4: numerical methods.

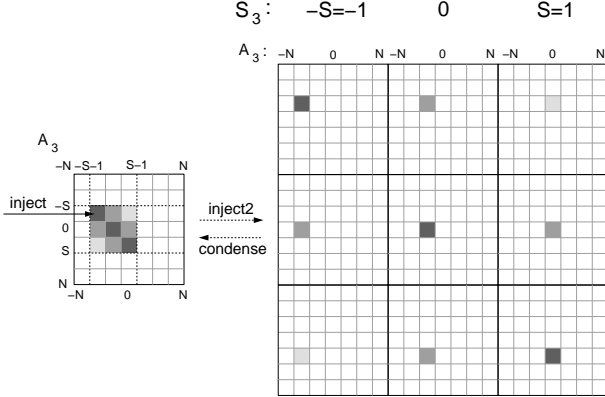


Fig.7. S_3 -extension of the algorithm.

The necessary extensions of the algorithms developed in Part II from $S = 0$ to $S > 0$ consist in the introduction of the additional block structure, related with the quantum number $S_3 \in [-S, S]$. Now we need to compute the matrix elements $\langle \chi_3 = 0, Q | \alpha_2 | \chi_3 = 1, Q \rangle$, shown on fig.7 at the right. Here the large blocks correspond to S_3 number, small blocks correspond to A_3 . The required matrix elements are localized in the intersection of rows with $-S \leq S_3 = A_3 \leq S$ and columns with $-S \leq S_3 = A_3 + 1 \leq S$. Actually, the only extension is required in the algorithm *ord*, procedure *inject*, see Part II. The results of sparse matrix multiplication after injection to $\langle A_{3f}, Q | \alpha_2 | A_{3i}, Q \rangle$ blocks in the left matrix on fig.7 should be further passed to the right matrix. However, keeping in this matrix only necessary elements, we condense it back to the smaller left matrix and perform the actual computations in it. Each monomial has a definite ΔA_3 -charge and therefore contributes to one of the diagonals in this matrix, marked on fig.7: $\langle S_3 = A_3 | mon \cdot S_+^{n(S_+)} S_-^{n(S_-)} | S_3 - n(S_-) + n(S_+), A_3 - n(S_-) + n(S_+) - 1 \rangle = \langle A_3 | mon | A_3 - n(S_-) + n(S_+) - 1 \rangle \cdot \langle S_3 - n(S_-) + n(S_+) | S_+^{n(S_-)} S_-^{n(S_+)} | S_3 \rangle$. The last matrix element gives coefficient $\prod_{S_3 - n(S_-) + n(S_+) < m \leq S_3 + n(S_+)} \sqrt{S(S+1) - m(m-1)}$ $\cdot \prod_{S_3 \leq m < S_3 + n(S_+)} \sqrt{S(S+1) - m(m+1)}$. Here in the case of empty set of indices (e.g. $n(S_+) = 0$) we define $\prod = 1$. If $S_3 + n(S_+) > S$ or $S_3 - n(S_-) + n(S_+) < -S$, we have $\prod = 0$. Substituting $S_3 = A_3$ in these formulae, we have non-zero coefficients only for the values $A_3 + n(S_+) \leq S$, $A_3 - n(S_-) + n(S_+) \geq -S$, i.e. A_3 changed between $A_{3min} = \max\{-S, -S + n(S_-) - n(S_+)\}$ and $A_{3max} = S - n(S_+)$. If $A_{3min} > A_{3max}$, the monomial is omitted. Then we initialize the sparse matrix multiplier as projector to $(A_3 \in [A_{3min}, A_{3max}], L_0^{(2)} \bmod 4 = Q)$ subspace and perform the rest computation as described in Part II. As an additional optimization, in the products $\prod_i op_i^{k_i}$ we have implemented preliminary computation and storage of the powers op_i^k for $k = 1 \dots kmax_i$, accelerating this procedure by a factor 1.8.

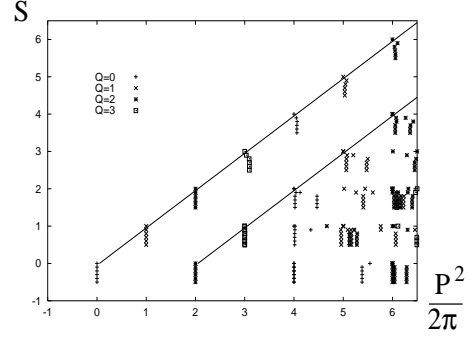


Fig.8. Spectrum $(P^2/2\pi, S - \epsilon n)$ as a function of n .

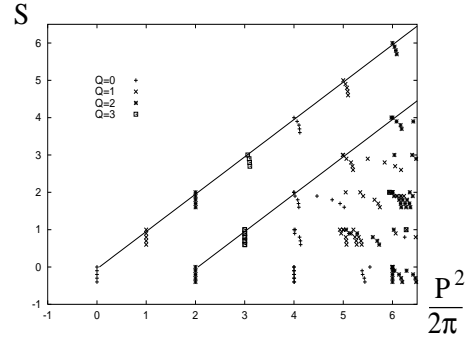


Fig.9. Spectrum $(P^2/2\pi, S - \epsilon N)$ as a function of N .

The determined spin-mass spectrum as a function of the correction order n and cutoff parameter N is presented on figs 8,9. The figure 8 shows superimposed spectra $(P^2/2\pi, S - \epsilon n)$ at fixed $N = 11$, where ϵ is a small constant and n is changed from 1 to 6 in the direction from top to bottom. By the reasons explained in the lemmas above, some of the states remain fixed (vertical) with the change of n , while the others are rapidly stabilized with n . On the figure 9 the spectra $(P^2/2\pi, S - \epsilon N)$ are shown for $n = 3$, $N = 7 \dots 20$, where in each Q -sector values $N \bmod 4 = Q$ were selected. When N increases, the most of the states also show tendency to stabilization. The spectrum, presented on fig.3, is computed for $n = 3$ and $N = 17, 18, 19, 20$ for 4 values of Q superimposed in this spectrum.

The other statistics of the algorithm is presented in the following tables:

Number of secondary monomials in each order $n = 1..6$						
n	1	2	3	4	5	6
num. of monomials	2	8	48	248	1066	3844

Time and memory requirements of the algorithm
($n = 3, S = 6, Q = 0$):

N	8	12	16	20
<i>subdim</i>	85×83	447×438	1932×1900	7288×7183
req.memory	2.1Mb	5.6Mb	83Mb	1.1Gb
comp.time	0.08 sec	1.4 sec	14 min	15 hours

In the last table *subdim* is the dimension of $S = 6, Q = 0$ block in dense matrices, which at large N mainly defines the amount of required memory. The computation is performed on HP 2GHz Linux PC.

This figure "grib.gif" is available in "gif" format from:

<http://arxiv.org/ps/hep-th/0306010v1>